VOLATILITY STUDIES OF THE S&P 500 INDEX

YANHUI LIU
Center for Polymer Studies and Department of Physics
Boston University, Boston, MA 02215, USA

PIERRE CIZEAU
Center for Polymer Studies and Department of Physics
Boston University, Boston, MA 02215, USA

PARAMESWARAN GOPIKRISHNAN
Center for Polymer Studies and Department of Physics
Boston University, Boston, MA 02215, USA

MARTIN MEYER
Center for Polymer Studies and Department of Physics
Boston University, Boston, MA 02215, USA

C.-K. PENG
Beth Israel Deaconess Medical Center
Harvard Medical School, Boston, MA 02215, USA

AND

H. EUGENE STANLEY
Center for Polymer Studies and Department of Physics
Boston University, Boston, MA 02215, USA

1. Introduction

Economic time series, as e.g., stock market indices or currency exchange rates depend on the evolution of a large number of strongly interacting systems far from equilibrium, and belong to the class of complex evolving systems [1], widely studied in physics and biology [2–4].

Thus, the statistical properties of financial markets have attracted the interest of many physicists [5–16]. Methods originating in statistical physics have been proven useful in analyzing financial indices. They are also used to construct new models for the pricing of derivatives and the assessment of the involved risk [8].

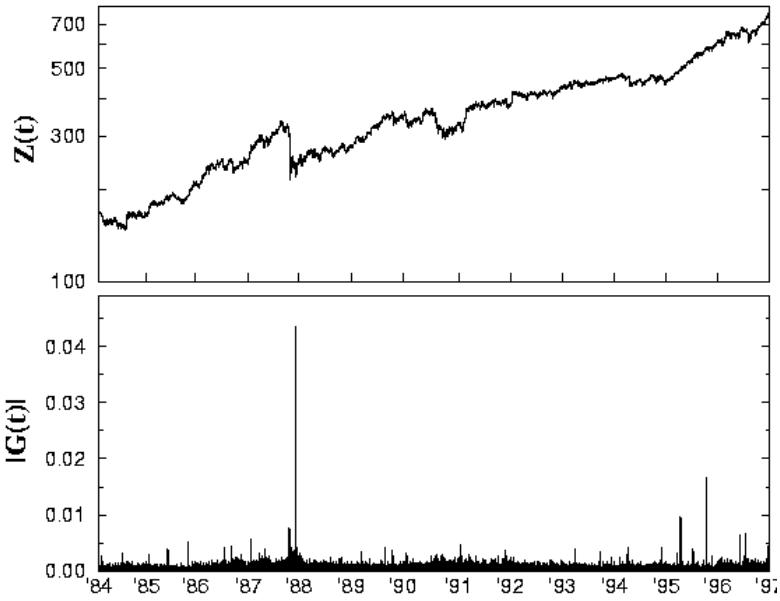

Figure 1. (a) Raw data analyzed: The S&P 500 index $Z(t)$ for the 13-year period 3 Jan 1984 – 31 Dec 1996 at intervals of 1 min (these data extend by 7 years the data set analyzed by Mantegna and Stanley [9]). Note the large fluctuations, such as that on 19 Oct 1987 ("black Monday"). (b) Amplitude of fluctuations $|G(t)|$, with $\Delta t = 1$ min. Notice the outliers in the $|G(t)|$ data correspondence to the big changes in the index.

The recent availability of very high frequency data allows us to study economic time series with a high accuracy on a wide range of time scales varying from less than 1 minute up to more than 10 years. Consequently, a large number of methods known from statistical physics have been applied to characterize the time evolution of stock prices and foreign exchange rates [5–9, 13–16]. It turns out that the distributions of the increments of economic time series, both in stock market indices and foreign currency exchange rates, are nearly symmetric and have strong "leptokurtic" wings [9, 17]. Index increments as a function of time show only weak correlations on short time scales below 10 minutes [17, 18], which seemingly makes them fundamentally different from well known examples of complex dynamic systems in physics such as, e.g., turbulent flow where power law correlations on long time scales are commonly observed [19].

The situation is different for the volatility, i.e. the market fluctuations averaged on a suitable time interval. There is long time persistence much larger than the correlation time in volatility [20]. Volatility is the key input

of virtually all option pricing models, including the classic Black and Scholes [21] and Cox, Ross, and Rubinstein [22] binomial models that are based on estimates of the asset's volatility over the remaining life of the option. So understanding the dynamics of the volatility has very important practical implications.

Here we quantify long range power law correlations in the volatility of the S&P 500 stock index and report the occurrence of a cross-over phenomenon of this long range correlation. Furthermore, we discuss the distribution of the volatility, and show that it can be fitted very well by a log-normal distribution.

2. Quantification of Correlations in S&P 500

2.1. DATA DESCRIPTION AND DETRENDING

The S&P 500 index, an index of the New York Stock Exchange, consists of the 500 largest companies in the US. It is a market-value weighted index (stock price times number of shares outstanding), with each stock's weight in the index proportionate to its market value. The S&P 500 index is one of the most widely used benchmarks of U.S. equity performance. Our data cover 13 years (from Jan 1984 to Dec 1996, see Fig. 1a), with a recording frequency of 15 seconds interval. The total number of data points in this 13 years period exceed 4.5 million, which allows for a very detailed statistical analysis.

Fig. 1a shows the S&P 500 index $Z(t)$ from 1984 to 1996 in semi-log graph. The index $Z(t)$ tends to increase constantly except some crashes, such as the crashes in Oct. 1987 and May 1990. Since the standard deviation of $Z(t+\Delta t)-Z(t)$ is proportional to the price level, we take the logarithm of the index as everyone does. We define the forward change $G(t)$ quantity in this paper

$$G(t) \equiv \log_e Z(t+\Delta t) - \log_e Z(t) \ , \tag{1}$$

where Δt is the time-lag (set to 1 minute in the correlation study).

We only count the number of minutes during the opening hours of the stock market, and remove the nights, weekends and holidays from the data set, i.e. the closing and the next opening of the market is continuous.

The absolute value of $G(t)$ describes the amplitude of the fluctuation, as shown in Fig. (1b). $|G(t)|$ is, by definition, always positive, and there are no obvious global trends visible, which is due to the logarithmic difference, i.e. the relative increment on the original index $Z(t)$. The large values of $Z(t)$ correspond to the crashes and big rallies of the index. It is known in the financial literature that the volatility varies in time [23], as expected the $|G(t)|$ quantity also fluctuates in time.

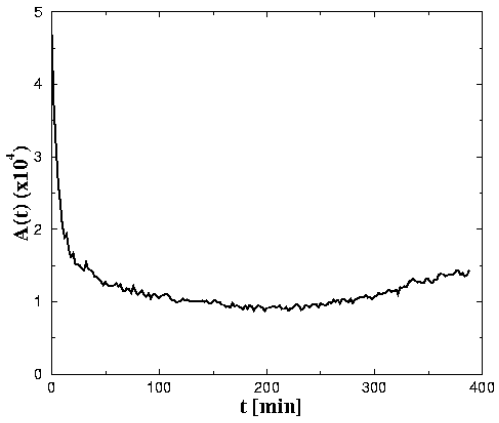

Figure 2. The intra-day pattern $A(t)$ of S&P 500 index marked by 1-minute interval. Before Sept. 30, 1985, the data length is 6 hours per day. After then, it's $6\frac{1}{2}$ hours. The two curves have the same pattern, only the latter curve is shown here. Big changes in the price happen within the first 10 minutes after the market opens.

It is known that there exist intra-day patterns in NYSE and S&P 500 index data, one simple explanation is that there are many information traders active near the opening and many liquidity traders active near the closing [24]. We find a similar intra-day pattern in our S&P 500 index data set(Fig. (2)). The intra-day pattern is defined as

$$A(t) \equiv \frac{\sum_{i=1}^{N} |G(t_{i,same})|}{N} , \tag{2}$$

where N is the total trading days over the 13-year period and t_{same} is the same time of each day ($N = 3309$ in our study). In order to avoid the artificial correlation caused by this daily oscillation, the $G(t)$ signal is normalized by the intra-day pattern

$$g(t) \equiv G(t)/A(t) , \tag{3}$$

i.e. each data point divided by the intra-day pattern of its corresponding time during the day.

2.2. METHODS TO CALCULATE CORRELATIONS

We have three methods to quantify the correlations. The direct method of studying the correlation property is the correlation function estimation, which is defined as

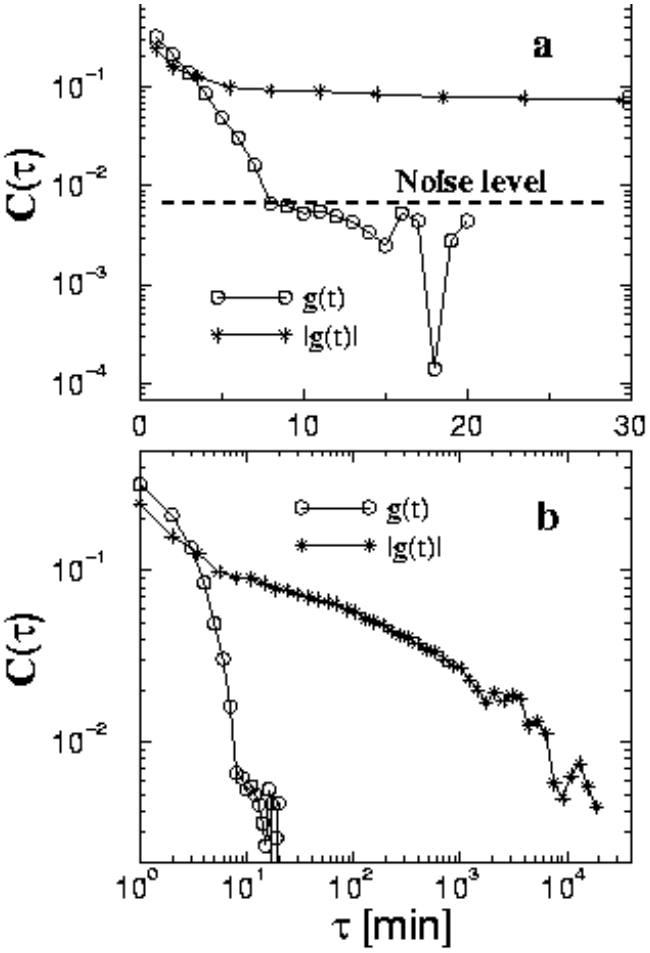

Figure 3. (a) Semi-log plot of correlation functions of $g(t)$ and $|g(t)|$. (b) The same correlations in the double log plot. $g(t)$ decays exponentially to 0 within half an hour. But the curve of $|g(t)|$ decays very slowly for more than 4 decades. A power law correlation seems to exist for $|g(t)|$. Note that both graphs are truncated at the first zero value of $C(\tau)$.

$$C(\tau) \equiv \frac{\langle G(t)G(t+\tau)\rangle - \langle G(t)\rangle^2}{\langle G^2(t)\rangle - \langle G(t)\rangle^2} \tag{4}$$

where τ is the time lag. The problem with the correlation function estimation is that it depends on the estimated average value of the time series. Since it is difficult to calculate the true average value, the correlation function can only give us a qualitative estimation [25].

Another method of calculating the correlation functions is the traditional power spectrum analysis. Since this method can only apply to linear and stationary (or strictly periodic) time series, although it could give quantitative measures, we still need some other method to confirm its results.

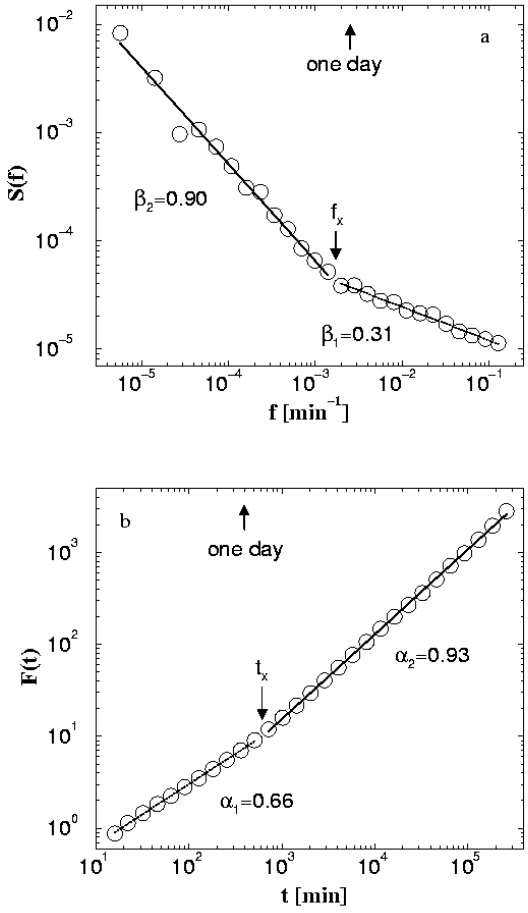

Figure 4. Plot of (a) the power spectrum $S(f)$ and (b) the detrended fluctuation analysis $F(t)$ of the absolute values of the 1 min increments. The lines show the best power law fits (r values are better than 0.99) to the data above and below the crossover frequency of $f_\times = (1/570)\,\mathrm{min}^{-1}$ in (a) and of the crossover time $t_\times = 600\,\mathrm{min}$ in (b). To remove artificial correlations resulting from the intra-day pattern of the market activity [24, 26–28], we analyze normalized data $|g(t)| \equiv |G(t)|/A(t)$, where $A(t)$ is the activity at the same time of the day averaged over all days of the data set. For the DFA method, we integrate $|g(t)|$ once; then we determine the fluctuations $F(t)$ of the integrated signal around the best linear fit in a time window of size t.

We applied the third method—termed *detrended fluctuation analysis*

(DFA) [29, 30]—-to quantify the correlation exponent. The advantages of DFA over conventional methods (e.g. spectral analysis and Hurst analysis) are that it permits the detection of long-range correlations embedded in a nonstationary time series, and also avoids the spurious detection of apparent long-range correlations that are an artifact of nonstationarities. This method has been validated on control time series that consist of long-range correlations with the superposition of a nonstationary external trend [29]. The DFA method has also been successfully applied to detect long-range correlations in highly complex heart beat time series [30, 31], and other physiological signals [32, 33].

A detailed description of the DFA algorithm appears elsewhere [29, 30]. Briefly, the $|g(t)|$ time series (with N data) is first integrated,

$$y(t) \equiv \sum_{i=1}^{t} |g(i)| \; . \tag{5}$$

Next the integrated time series is divided into boxes of equal length, n. In each box of length n, a least squares line is fit to the data (representing the *trend* in that box). The y coordinate of the straight line segments is denoted by $y_n(t)$. Next we detrend the integrated time series, $y(t)$, by subtracting the local trend, $y_n(t)$, in each box. The root-mean-square fluctuation of this integrated and detrended time series is calculated by

$$F(n) = \sqrt{\frac{1}{N} \sum_{t=1}^{N} [y(t) - y_n(t)]^2}. \tag{6}$$

This computation is repeated over all time scales (box sizes) to provide a relationship between $F(n)$, the average fluctuation as a function of box size. In our case, the box size n ranged from 10 min to 10^5 min, the upper bound of n is determined by the actual data length. Typically, $F(n)$ will increase with box size n (Fig. 4b). A linear relationship on a double log graph indicates the presence of power law (fractal) scaling. Under such conditions, the fluctuations can be characterized by a scaling exponent α, the slope of the line relating $\log F(n)$ to $\log n$ (Fig. 4b).

For exactly self-similar process, as e.g. fractional Brownian motion, the DFA exponent α is related to the power spectrum exponent β through the relation $\alpha = (1 + \beta)/2$ [25]. The calculation of $F(n)$ can distinguish four types of behavior. (1) Uncorrelated time series give rise to uncorrelated random walks described by $F(n) \sim n^{\alpha}$ with $\alpha = 1/2$, as expected from the central limit theorem. The power spectrum would be flat with $\beta = 0$. (2) Markov processes with a characteristic correlation length t_0 give $C(\tau) \sim exp(-\tau/t_0)$; for $t < t_0$, it is the Brownian process with $\alpha = 1.5$ and

corresponding $\beta = 2$, nonetheless the asymptotic behavior for sufficiently large t with $\alpha = 1/2$ would be unchanged from the purely random case. (3) In the presence of long-range correlations with no characteristic time scale, the scaling property would be a power law function with $\alpha \neq 1/2$ and $\beta \neq 0$.

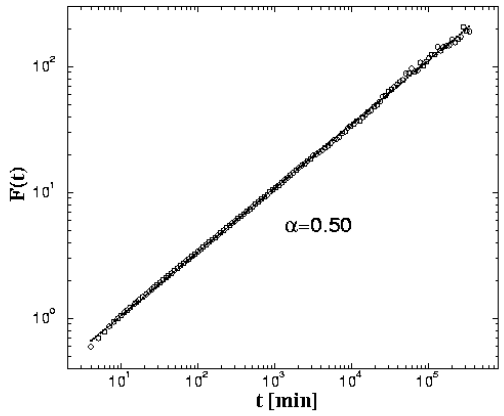

Figure 5. Double log plot of the DFA measurement of randomly shuffled $|g(t)|$ time series. Circles are the fluctuations of the data, the least square fitting gives DFA exponent $\alpha = 0.50$, which means that no correlation exists.

2.3. CORRELATION RESULTS OF S&P 500 INDEX

Using correlation function estimation, we find that the correlation function of $g(t)$ decays exponentially with a characteristic time of the order of 1-10 min, but the absolute value $|g(t)|$ does not (Fig. 3). This result is consistent with previous studies on several economic series [18, 20, 34].

The power spectrum calculation of $|g(t)|$ (Fig. 4a) shows that the data fit not one but rather two separate power laws: for $f > f_\times$ the power law exponent is $\beta_1 = 0.31$, while for $f < f_\times$ the exponent $\beta_2 = 0.90$ is three times larger; here $f_\times$ is called the crossover frequency.

DFA method confirms our power spectrum results (Fig. 4a). From the behavior of the power spectrum, we expect that the DFA method will also predict two distinct regions of power law behavior, with exponents $\alpha_1 = 0.66$ and $\alpha_2 = 0.95$ for t less than or greater than a characteristic time scale $t_\times \equiv 1/f_\times$, where we have used the relation

$$\alpha = (1 + \beta)/2 \, . \tag{7}$$

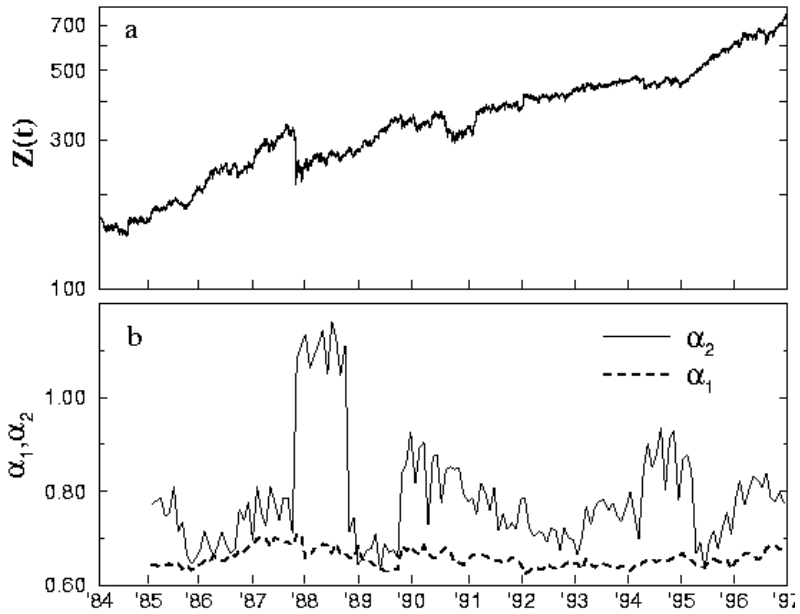

Figure 6. (a) Raw data analyzed: The S&P 500 index $Z(t)$ for the 13-year period These data extend by 7 years the data set analyzed by Mantegna and Stanley [9]. (b) Results of dragging a window of size 1 y down the same data base, one month at a time, and calculating the best fit exponent α_1 (dashed line) and α_2 (full line) for the time intervals $t < t_\times$ and $t > t_\times$ respectively.

The data of Fig. 4b yield $\alpha_1 = 0.66$, $\alpha_2 = 0.93$, thereby confirming the consistency of the power spectrum and DFA methods. Also the crossover time is very close to the result obtained from the power spectrum, with

$$t_\times \approx 1/f_\times \approx 600\,\mathrm{min} \tag{8}$$

it is about 1.5 trading days.

To test whether this correlation is due to the distribution function, we shuffled each point of the $|g(t)|$ time series randomly. The shuffling operation keeps the distribution of $|g(t)|$ unchanged, but kills the correlations in the time series totally if there are any. DFA measurement of this randomly shuffled data does not show any correlations and gives exponent $\alpha = 0.50$ (Fig. 5). This tells us that the long-range correlations are actually due to the dynamics of the economic system and not simply due to the distribution.

The observed long range correlation and the crossover behavior noted above is from the entire 13-year period, so it is natural to enquire whether it will still hold for periods smaller than 13 years. Therefore, we choose

a sliding window (with size 1 y) and calculate both exponents α_1 and α_2 within this window as the window is dragged down the data set with one month step. We find (Fig. 6b) that the value of α_1 is very "stable" (independent of the position of the window) fluctuating around the mean value 2/3. Surprisingly, however, the variation of α_2 is much greater, showing sudden jumps when very volatile periods enter or leave the time window.

We studied several standard mathematical models, such as fractional Brownian motion [25, 35] and fractional ARIMA processes [36], commonly used to account for long-range correlation in a time series and found that none of them can reproduce the large fluctuation of α_2.

3. The Volatility Distribution of S&P 500

The volatility is a measure of the mean fluctuation of a market price over a certain time interval T. The volatility is of practical importance since it quantifies the risk related to assets [8]. As shown above, unlike price changes that are correlated only on very short time scales [18] (a few minutes), the absolute values of price changes (which are closely related to the volatility) show correlations on time scales up to many years [20, 34, 37, 38].

The same data set of the S&P 500 index of the New York stock exchange is explored here to study the volatility distribution. This data set has been extended by 7 years from the data set previously analyzed in [9].

We calculate the logarithmic increments $G(t)$ in Eq. 1, where $G(t)$ is the relative price change $\Delta Z/Z$ in the limit $\Delta t \to 0$. Here we set $\Delta t = 30\,\mathrm{min}$, well above the correlation time of the price increments; and we obtain similar results for other choices of Δt (larger than the correlation time).

As we showed in the correlation discussion, there is a strong "U-shape" market activity over the day. To remove artificial correlations resulting from this intra-day pattern of the volatility [26–28, 39], we normalized $|G(t)|$ by $A(t)$ as shown in Eq. 3.

We obtain the volatility at a given time by averaging $|g(t)|$ over a time window $T = n \cdot \Delta t$ with some integer n,

$$v_T(t) \equiv \frac{1}{n} \sum_{t'=t}^{t+n-1} |g(t')| \,. \tag{9}$$

Fig. 7 shows (a) the S&P500 index and (b) the signal $v_T(t)$ for a long averaging window $T = 8190\,\mathrm{min}$ (about 1 month). The volatility fluctuates strongly showing a marked maximum for the '87 crash. In general, periods of high volatility are not independent but tend to "cluster". This clustering is especially marked around the '87 crash, which is accompanied by precursors (possibly related to the oscillatory patterns postulated in [8]). Clustering occurs also in other periods (e.g. in the second half of '90), while there are

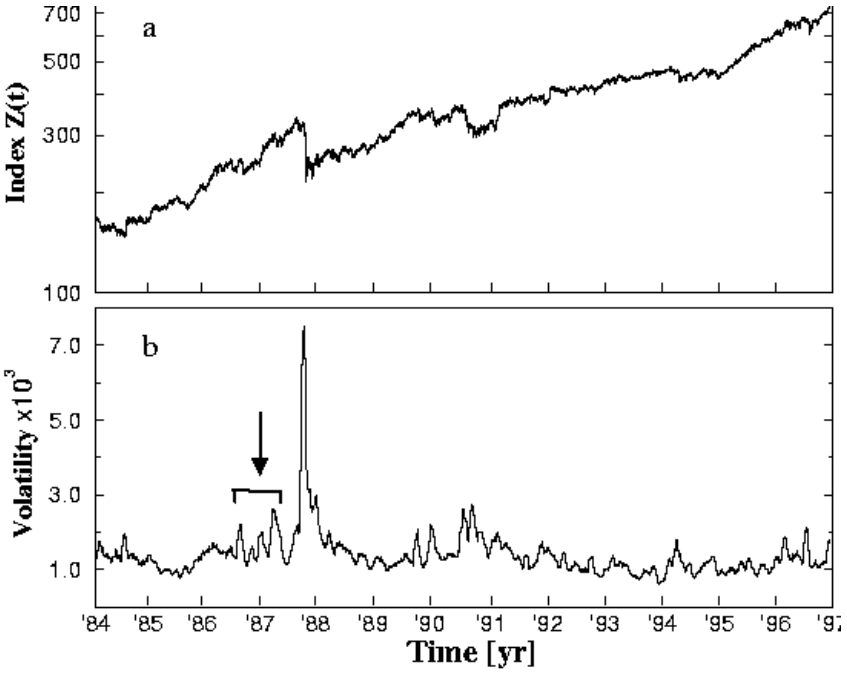

Figure 7. (a) Raw data analyzed: The S&P 500 index Z(t) for the 13-year period. (b) Volatility $v_T(t)$ with T=1 month (8190min) and time lag 30min. Possible "precursors" of the '87 crash are indicated by arrows.

extended periods where the volatility remains at a rather low level (e.g. the years of '85 and '93).

Fig. 8a shows the scaled probability distribution $P(v_T)$ for several values of T. The data for different averaging windows collapse to one curve. Remarkably, the scaling form is log-normal, not Gaussian. In the limit of very long averaging times, one expects that $P(v_T)$ will become Gaussian, since the central limit theorem also holds for correlated series [25], with a slower convergence than for non-correlated processes [12, 40]. However, a log-normal fits the data better than a Gaussian, as is evident in Fig. 8b which compares the best log-normal fit with the best Gaussian fit for data averaged over a 300 min window.

The correlations found in Fig. 7b can be accurately quantified by detrended fluctuation analysis [29]. The analysis reveals power-law behavior independent of the T value chosen (Fig. 9) with an exponent $\alpha \cong 0.9$ in agreement with the value found for the absolute price increments (see Sec. 2).

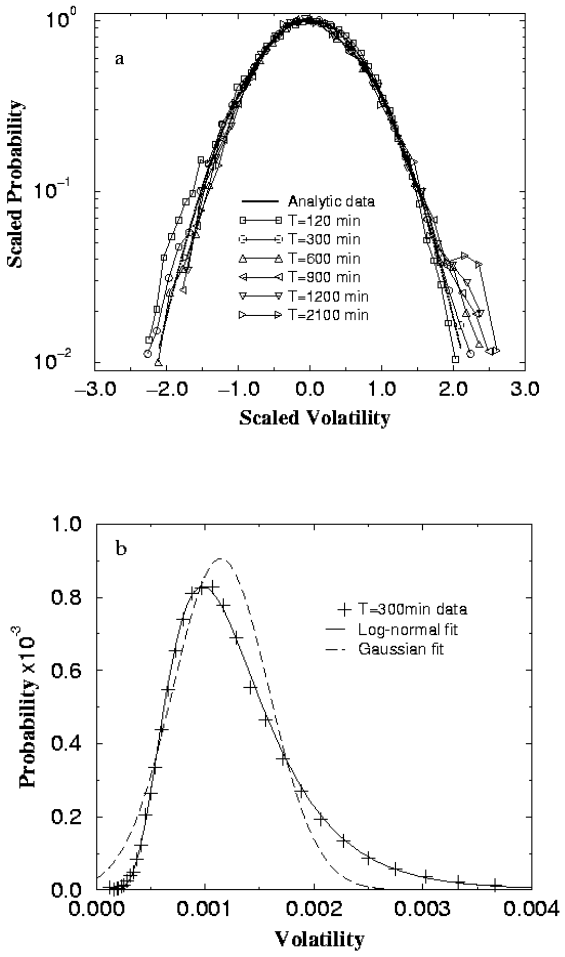

Figure 8. (a) The volatility distribution for different window sizes T in scaled form, $\sqrt{\mu}\exp(a+\mu/4)P(v_T)$ as a function of $(\ln(v_T)-a)/\sqrt{\pi\mu}$, where a and μ are the mean and the width on a logarithmic scale. By the scaling, all curves collapse to the log-normal form with $a=0$ and $\mu=-1$, $\exp(-(\ln x)^2)$ (dotted line). (b) Comparison of the best log-normal and Gaussian fits for the 300min data.

4. Discussion of Empirical Results

In this study, we have used the DFA method to display correlation in the volatility of S&P 500 index. We find that the volatility is highly correlated, and that the correlation is remarkably long range, indeed, over 5 decades. Moreover, the quantitative scaling of the correlation follows the power law form observed in numerous phenomena which have a self-similar or "fractal"

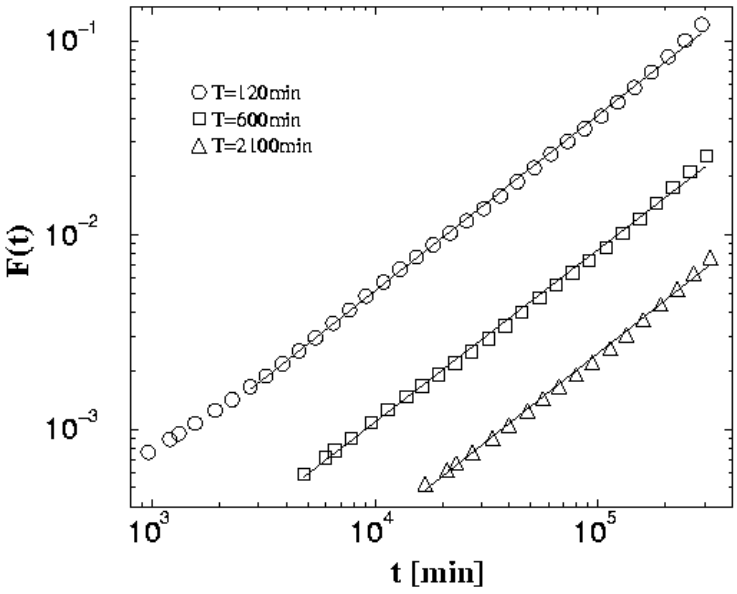

Figure 9. The fluctuation $F(t)$ of volatility $v_T(t)$ with T=120 min, 600 min, and 2100 min, calculated using detrended fluctuation analysis (DFA) [29]. To implement the DFA method, we integrate $v_T(t)$ once; then we determine the fluctuations $F(t)$ of the integrated signal around the best linear fit in a time window of size t. The lines are the best power-law fits with exponents α =0.91, 0.89, and 0.91.

origin.

We have also found that the probability distribution of the S&P500 volatility can be well described by a log-normal function. This functional shape does not depend on the averaging time interval T used to calculate volatility $v_T(t)$. The log-normal shape of the distribution is consistent with a multiplicative process [41] for the volatility [10]. However, a multiplicative behavior would be surprising, because efficient market theories [18] assume that the price reflects all current information that could anticipate future events and the price changes, $G(t)$, are caused by incoming new information about an asset. Since such information-induced price changes are additive in $G(t)$, they should not give rise to multiplicative behavior of the volatility.

To account for the time dependence of the volatility and its long-range correlations, ARCH [42], GARCH [43] models and related approaches [36] have been developed, which assume that the volatility depends on time and on the past evolution of the index. It may also be worthwhile testing these models with regard to the volatility distribution $P(v_T)$.

5. Acknowledgments

We thank S. Havlin, R. Mantegna, and S. Zapperi for very helpful discussions through the course of this work, and DFG, NIH, and NSF for financial support.

References

1. P. W. Anderson, K. J. Arrow and D. Pines, *The Economy as an Evolving Complex System* (Addison-Wesley, Redwood City, 1988).
2. C.-K. Peng, S. Buldyrev, A. Goldberger, S. Havlin, F. Sciortino, M. Simons and H. E. Stanley, *Nature* **356**, 168–171 (1992).
3. H. Makse, S. Havlin and H. E. Stanley, *Nature* **377**, 608–612 (1995).
4. H. E. Stanley, L. A. N. Amaral, S. V. Buldyrev, A. L. Goldberger, S. Havlin, H. Leschhorn, P. Maass, H. Makse, C.-K. Peng, M. A. Salinger, M. H. R. Stanley and G. M. Viswanathan, *Physica A* **231**, 20–48 (1996), and references therein.
5. P. Bak, K. Chen, J. A. Scheinkman and M. Woodford, *Richerche Economichi* **47**, 3 (1993); J. A. Scheinkman and J. Woodford, *American Economic Review* **84**, 417 (1994).
6. M. H. R. Stanley, L. A. N. Amaral, S. V. Buldyrev, S. Havlin, H. Leschhorn, P. Maass, M. A. Salinger, and H. E. Stanley, *Nature* **379**, 804 (1996).
7. M. Levy, H. Levy, and S. Solomon, *Economics Letters* **45**, 103 (1994).
8. J.-P. Bouchaud and D. Sornette, *J. Phys. I (France)* **4**, 863 (1994); D. Sornette, A. Johansen, and J.-P. Bouchaud, *J. Phys. I (France)* **6**, 167 (1996).
9. R. N. Mantegna and H. E. Stanley, *Nature* **376**, 46 (1995).
10. S. Ghashghaie, W. Breymann, J. Peinke, P. Talkner, and Y. Dodge, *Nature* **381**, 767 (1996); see also R. N. Mantegna and H. E. Stanley, *Nature* **383**, 587 (1996); *Physica* A **239**, 255 (1997) and A. Arneodo et al. (preprint).
11. M. Levy and S. Solomon, "Power laws are logarithmic Boltzmann laws" (preprint, 1996).
12. M. Potters, R. Cont, J.-P. Bouchaud, "Financial markets as adaptative systems" (preprint, 1996).
13. H. Takayayasu, H. Miura, T. Hirabayashi, and K. Hamada, *Physica A* **184**, 127–134 (1992).
14. T. Hirabayashi, H. Takayayasu, H. Miura, and K. Hamada, *Fractals* **1**, 29–40 (1993).
15. H. Takayasu and K. Okuyama, *Fractals* (to appear).
16. P. R. Krugman, *The Self-Organizing Economy* (Blackwell Publishers, Cambridge, 1996).
17. B. B. Mandelbrot, *J. Business* **36**, 393 (1963).
18. E.-F. Fama, *J. Finance* **25**, 383 (1970).
19. A. N. Kolmogorov. Local structure of turbulence in fluid for very large Reynolds numbers. In *Transl in Turbulence.* S. K. Friedlander and L. Topper, eds. (Interscience Publishers, New York, 1961), pp. 151–155.
20. Z. Ding, C. W. J. Granger and R. F. Engle, *J. Empirical Finance* **1**, 83 (1983).
21. F. Black and M. Scholes, *J. of Political Economy* **81**, 637 (1973).
22. J. Cox, S. Ross and M. Rubinstein, *J. of Financial Economics* **7**, 229 (1979).
23. T. Bollerslev, R. Y. Chou, and K. F. Kroner, *J. Econometrics* **52**, 5 (1992); G. W. Schwert, *The Journal of Finance* **44**, 1115 (1989); A. R. Gallant, P. E. Rossi and G. Tauchen, *The Review of Financial Studies* **5**, 199 (1992); B. Le Baron, *Journal of Business* **65**, 199 (1992); K. Chan, K. C. Chan and G. A. Karolyi *The Review of Financial Studies* **4**, 657 (1991).
24. A. Admati and P. Pfleiderer, *Review of Financial Studies* **1**, 3 (1988).

25. J. Beran, *Statistics for Long-Memory Processes* (Chapman & Hall, NY, 1994).
26. R. A. Wood, T. H. McInish and J. K. Ord, *J. of Finance* **40**, 723 (1985).
27. L. Harris, *J. of Financial Economics* **16**, 99 (1986).
28. P. D. Ekman, *The Journal of Futures Markets* **12**, 365 (1992).
29. C.-K. Peng, S. V. Buldyrev, S. Havlin, M. Simons, H. E. Stanley and A. L. Goldberger, *Phys. Rev.* E **49**, 1684 (1994).
30. C.-K. Peng, S. Havlin, H. E. Stanley, A. L. Goldberger. *CHAOS* **5**, 82–87 (1995).
31. N. Iyengar, C.-K. Peng, R. Morin, A. L. Goldberger, L. A. Lipsitz. *Am. J. Physiol.* **271**, R1078–R1084 (1997).
32. J. M. Hausdorff, P. L. Purdon, C.-K. Peng, Z. Ladin, J. Y. Wei, A. L. Goldberger. *J. Appl. Physiol.* **80**, 1448–1457 (1996).
33. J. M. Hausdorff, C.-K. Peng. *Phys Rev E* **54**, 2154–2157 (1996).
34. M. M. Dacorogna, U. A. Muller, R. J. Nagler, R. B. Olsen and O. V. Pictet, *J. International Money and Finance* **12**, 413 (1993).
35. B. B. Mandelbrot and J. W. van Ness, *SIAM Rev.* **10**, 422 (1968).
36. C. W. J. Granger and Z. Ding, *J. Econometrics* **73**, 61 (1996).
37. Y. Liu, P. Cizeau, M. Meyer, C.-K. Peng, and H. E. Stanley, *Physica* A **245**, 437 (1997).
38. P. Cizeau, Y. Liu, M. Meyer, C.-K. Peng, and H. E. Stanley, *Physica* A **245**, 441 (1997).
39. A. Admati and P. Pfleiderer, *Review of Financial Studies* **1**, 3 (1988).
40. R. Cont, cond-mat/9705075
41. A. Bunde and S. Havlin, in *Fractals and Disordered Systems*, ed. by A. Bunde and S. Havlin, 2nd ed. (Springer, Heidelberg 1996).
42. R. F. Engle, *Econometrica* **50**, 987 (1982).
43. T. Bollerslev, *J. Econometrics* **31**, 307 (1986).